

UC Santa Cruz

UC Santa Cruz Previously Published Works

Title

Optimized Merger of Ocean Chlorophyll Algorithms of MODIS-Aqua and VIIRS

Permalink

<https://escholarship.org/uc/item/6rn5657w>

Journal

IEEE Geoscience and Remote Sensing Letters, 12(11)

ISSN

1545-598X

Authors

Kahru, Mati
Kudela, Raphael M
Anderson, Clarissa R
et al.

Publication Date

2015-11-01

DOI

10.1109/lgrs.2015.2470250

Peer reviewed

Optimized Merger of Ocean Chlorophyll Algorithms of MODIS-Aqua and VIIRS

Mati Kahru, Raphael M. Kudela, Clarissa R. Anderson, and B. Greg Mitchell

Abstract—Standard ocean chlorophyll-a (Chla) products from currently operational satellite sensors Moderate Resolution Imaging Spectroradiometer (MODIS) Aqua and Visible Infrared Imager Radiometer Suite (VIIRS) underestimate medium and high *in situ* Chla concentrations and have approximately 9% bias between each other in the California Current. By using the regional optimization approach of Kahru *et al.*, we minimized the differences between satellite estimates and *in situ* match-ups as well as between estimates of the two satellite sensors and created improved empirical algorithms for both sensors. The regionally optimized Chla estimates from MODIS-Aqua and VIIRS have no bias between each other, have improved retrievals at medium to high *in situ* Chla, and can be merged to improve temporal frequency and spatial coverage and to extend the merged time series.

Index Terms—Chlorophyll, Moderate Resolution Imaging Spectroradiometer (MODIS), ocean color, phytoplankton, Visible Infrared Imager Radiometer Suite (VIIRS).

I. INTRODUCTION

COMBINING or merging data from multiple sensors is required to improve the temporal resolution and spatial coverage of ocean color imagery and to construct long time series or climate data records using data from multiple sensors [2]–[5]. Currently (i.e., in mid-2015), there are two well-calibrated global ocean color sensors in operation: Moderate Resolution Imaging Spectroradiometer on Aqua (MODISA) and Visible Infrared Imager Radiometer Suite (VIIRS) on Suomi NPP. While improvements in on-orbit sensor calibration [6] have greatly improved the compatibility between data from different sensors, significant differences remain [7], [8]. Moreover, global algorithms may not be regionally optimal as significant differences exist in bio-optical properties of different oceanic provinces [9]. Standard NASA ocean chlorophyll-a (Chla) algorithms significantly underestimate *in situ* values in the California Current at high concentrations, often by a factor

of 5 [1]. This is highly relevant for detection and monitoring of phytoplankton blooms, including harmful algal blooms [10]. While differences between Chla estimates from MODIS-Aqua and VIIRS have diminished after multiple reprocessings, they still exist [8].

Kahru *et al.* [1] created optimized empirical algorithms for the California Current for a suite of four sensors (OCTS, SeaWiFS, MERIS, and MODISA) and the time period of 1997–2011. An update to that work is currently needed as 1) MERIS stopped operating in April 2012; 2) new data from VIIRS are available from the beginning of 2012; and 3) both MODISA and VIIRS data have been reprocessed by NASA's Ocean Biology Processing Group. The purpose of this work is to create empirical algorithms that are optimized for creating a merged Chla time series in the California Current for the period of 2012–2015 from the two currently available sensors MODISA and VIIRS.

II. DATA AND METHODS

We used *in situ* Chla data collected by the California Cooperative Oceanic Fisheries Investigations (CalCOFI) on their quarterly cruises covering a regular grid of stations from nearshore to as far as 600 km offshore for the entire coast of California [11]. In total, 3388 near-surface Chla samples from 2002–2014 were used to validate MODISA data, and 744 Chla samples from 2012–2014 were used to validate VIIRS data.

All satellite data were acquired at level 2 (i.e., processed to surface quantities but unmapped) with approximately 1-km ground resolution. MODISA (2002–2014, version 2013.1.1) and VIIRS (2012–2014, version 2014.0.1) level-2 data were obtained from NASA's Ocean Color Web (<http://oceancolor.gsfc.nasa.gov/>). The standard NASA Chla algorithm uses empirical polynomial fits between satellite-derived maximum band ratio (MBR) of remote sensing reflectance (R_{rs}) bands and near-surface Chla [12] with the coefficient values for each sensor given at http://oceancolor.gsfc.nasa.gov/cms/atbd/chlor_a.

The validation of satellite products using quasi-simultaneous and spatially collocated measurements (match-ups) of satellite and *in situ* data followed the procedures of previous studies [1], [8], [13], [14]. We assumed that the following level-2 flags made a pixel invalid: ATMFAIL, LAND, HISATZEN, STRAYLIGHT, CLDICE, CHLFAIL, SEAICE, NAVFAIL, and HIPOL (see <http://oceancolor.gsfc.nasa.gov/VALIDATION/80flags.html> for an explanation of the flags). All variables in the level-2 files were extracted from a 3×3 -pixel window centered at the pixel nearest to the *in situ* sample. For statistical analysis, we accepted only those match-ups with at least five

Manuscript received May 28, 2015; revised July 9, 2015; accepted August 17, 2015. This work was supported by the NASA Ocean Biology and Biogeochemistry Program Grants NNX09AT01G (M. Kahru and R. M. Kudela), NNX13AL28G (C. R. Anderson, R. M. Kudela, and M. Kahru), and NNX14AC42G (C. R. Anderson and R. M. Kudela) and by the National Science Foundation (Grant OCE-1026607 to the CCE-LTER Program).

M. Kahru and B. G. Mitchell are with Scripps Institution of Oceanography, University of California, San Diego, La Jolla, CA 95064 USA (e-mail: mkahru@ucsd.edu; gmitchell@ucsd.edu).

R. M. Kudela and C. R. Anderson are with the Ocean Sciences Department, University of California, Santa Cruz, Santa Cruz, CA 95064 USA (e-mail: kudela@ucsc.edu; clrande@ucsc.edu).

Color versions of one or more of the figures in this paper are available online at <http://ieeexplore.ieee.org>.

Digital Object Identifier 10.1109/LGRS.2015.2470250

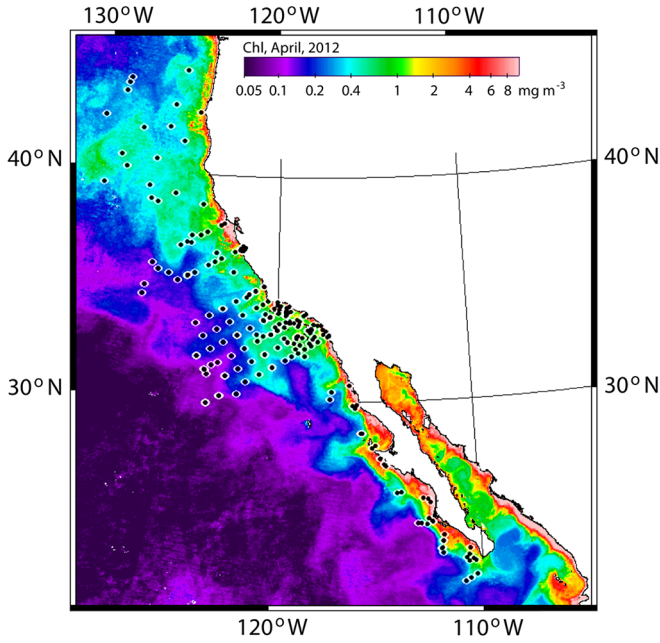


Fig. 1. Locations of the MODIS-Aqua Chla match-ups (black dots with white circles) within 3-h time difference overlaid on the April 2012 Chla composite.

85 valid pixels (out of nine). The maximum temporal difference 86 between satellite and *in situ* measurements was set at 3 h. 87 Satellite match-ups with high variability within the 3×3 -pixel 88 window were excluded if $(\text{Max} - \text{Min})/\text{Min} > 0.6$ for the 89 standard Chla variable *chlora*. The arithmetic mean Chla value 90 of all valid pixels within the 3×3 -pixel window was used as the 91 satellite retrieval. The spatial distribution of MODISA match- 92 ups with *in situ* measurements of Chla is shown in Fig. 1.

93 Satellite-derived *Rrs* values between different sensors are 94 difficult to compare at level 2, i.e., without remapping to a com- 95 mon map. Although both MODISA and VIIRS have equatorial 96 crossing times at approximately 1:30 P.M., their pixel-to-pixel 97 comparison at a spatial resolution of $\sim 1 \text{ km}^2$ corresponding 98 to their level-2 data shows high variability [8]. We therefore 99 used spatially binned and averaged *Rrs* values over a grid of 100 1° latitude \times 1° longitude covering an approximately 1000-km- 101 wide area along the coast extracted from daily NASA level-3 102 datasets. Those daily mean *Rrs* values of MODISA and VIIRS 103 were then matched with each other. In order to eliminate cloud 104 edges and coastal zones, we kept only those matching *Rrs* pairs 105 with at least 99% of the pixels within each $1^\circ \times 1^\circ$ subarea 106 having valid values. As a result, a total of 4060 matching *Rrs* 107 vectors for MODISA and VIIRS were found for the period 108 of 2012–2014. These MODISA to VIIRS match-ups were 109 then used in the minimization of the differences in the Chla 110 algorithm between MODISA and VIIRS.

111 Several statistical measures were used to assess the per- 112 formance of satellite products against *in situ* observations 113 and between different satellite sensors. For satellite to *in situ* 114 match-ups, we assume that O_i is the i th observation of an *in situ* 115 variable and P_i is the corresponding predicted satellite variable. 116 For sensor-to-sensor match-ups, the choice of the observed 117 versus predicted variable is arbitrary, but we used MODISA 118 estimates as O_i . As an estimate of the prediction scatter, we

TABLE I
STATISTICS FOR MATCH-UPS OF THE NASA STANDARD *chlora* PRODUCT WITH *In Situ* CHLA WITH UP TO 3-h TIME DIFFERENCE AND AT LEAST FIVE VALID PIXELS. N = NUMBER OF MATCH-UPS, R^2 = COEFFICIENT OF DETERMINATION, MDAPE = MEDIAN ABSOLUTE PERCENT ERROR, MDRPE = MEDIAN RELATIVE PERCENT ERROR, RMSE = ROOT MEAN SQUARE ERROR, AND RMA SLOPE = SLOPE OF THE RMA LINEAR REGRESSION

Sensor	N	R^2	MdAPE	MdRPE	RMSE	RmaSlope
MODISA	306	0.87	22.5	-0.1	0.15	0.88
VIIRS	74	0.85	31.0	8.0	0.21	0.68

used the median absolute percentage error (MdAPE), which 119 was calculated as $\text{MdAPE} = 100 \times \text{median} (|(P_i - O_i)/O_i|)$. 120 For comparing two sensors, we used the median unbiased 121 absolute percentage error (MdUAPE), which was calculated as 122 $\text{MdUAPE} = 100 \times \text{median} (|(P_i - O_i)/[0.5*(P_i + O_i)]|)$. As 123 an estimate of bias, we used the median relative percentage 124 error (MdRPE), which was calculated as $\text{MdRPE} = 100 \times$ 125 $\text{median} ((P_i - O_i)/O_i)$. These statistics were calculated for 126 P_i and O_i using untransformed values (i.e., not \log_{10}). We 127 also include the coefficient of determination (R^2), the slope 128 of the reduced major axis (RMA) regression, and the root- 129 mean-square error (rmse), all calculated on \log_{10} -transformed 130 variables. 131

III. RESULTS 132

A. Match-Ups With Standard *chlora* Products 133

Satellite to *in situ* match-ups of Chla using the NASA stan- 134 dard *chlora* product over three orders of magnitude (Fig. 2 and 135 Table I) have relatively high coefficients of determination 136 ($R^2 = 0.87$ for MODISA and 0.85 for VIIRS) but also show 137 bias. For example, all MODISA match-ups with *in situ* Chla $>$ 138 2 mg m^{-3} underestimate *in situ* Chla. For VIIRS, the standard 139 *chlora* product suffers from overestimation at low *in situ* Chla 140 and underestimation at medium and high Chla, which causes 141 the slope of the RMA regression to be significantly less than 142 one (0.68; Table I). 143

B. Optimized MBR Algorithm 144

Standard empirical ocean color algorithms OC3 and OC4 145 [12] use polynomial fits between \log_{10} -transformed *in situ* 146 Chla (Cins) and \log_{10} -transformed MBR of *Rrs* measured 147 *in situ*. MBR is calculated as the maximum of *Rrs* at two or 148 more wavelengths (e.g., *Rrs*443 and *Rrs*488 for MODISA or 149 *Rrs*443 and *Rrs*486 for VIIRS) to the *Rrs* of the green band 150 (*Rrs*547 for MODISA and *Rrs*551 for VIIRS). In order to 151 remove the bias evident in Fig. 2, we created our own best 152 fits to the match-up points. The distribution of match-up points 153 is highly uneven as there are more points in the middle of the 154 range than at both ends of the distribution. To reduce the effect 155 of the uneven distribution, the match-up points were aggregated 156 into bins by using the median values of small brackets of 157 $\log_{10}(\text{Cins})$ and the corresponding medians of $\log_{10}(\text{MBR})$ 158 following [3] and binning interval of 0.04 in $\log_{10}(\text{MBR})$ units. 159

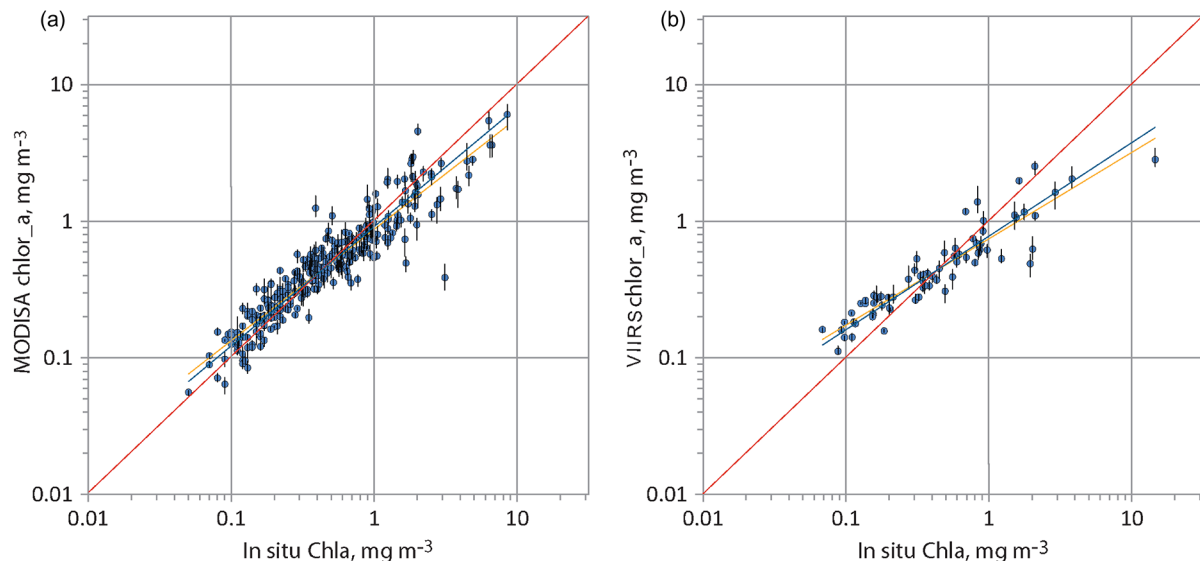


Fig. 2. Chlorophyll-a match-ups with (a) MODISA and (b) VIIRS using standard NASA *chlor_a* products. The red line is the one-to-one line, and the blue line is the RMA linear regression.

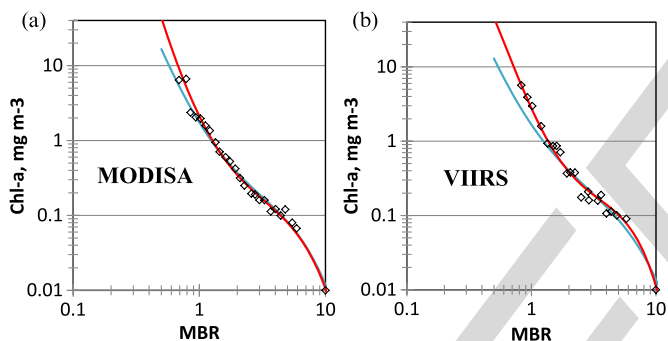


Fig. 3. Optimized Chla algorithm (red) compared to standard NASA OC3 (blue) and bracket points of *in situ* Chla match-ups (black diamonds) as a function of the MBR of remote sensing reflectance for (a) MODISA and (b) VIIRS.

160 The resulting “bracket” points (24 for MODISA and 20 for
161 VIIRS) were then used in algorithm development (Fig. 3).

162 Ideally, by “tuning” the algorithms of multiple sensors to the
163 same set of *in situ* data, the resulting estimates by different
164 sensors should be compatible between each other. In reality, as
165 the Chla high end is poorly constrained due to few scattered
166 match-ups, the resulting empirical algorithms do not improve
167 the intersensor consistency and may even make it worse [1].
168 Indeed, as the main difference of the empirical fits compared
169 to the standard OC3 algorithms is their increased predicted
170 Chla at high end (Fig. 3), the intersensor variability (MdAPE)
171 between MODISA and VIIRS is slightly increased from 13.7%
172 to 14.0% when using the coefficients fitted to *in situ* data
173 (Table II). In order to improve the consistency between satellite
174 sensors and at the same time keep them consistent with *in situ*
175 datasets, we need an optimization that minimizes not only the
176 differences between satellite and *in situ* match-ups but also the
177 differences between the satellite estimates of different sensors
178 [1]. The matching *Rrs* pairs of MODISA and VIIRS in $1^\circ \times 1^\circ$
179 subareas were further binned according to the corresponding
180 $\log_{10}(\text{MBR})$ value, which resulted in 89 “bracket points” of
181 MODISA and VIIRS $\log_{10}(\text{MBR})$ values. The differences in

TABLE II
STATISTICS OF VIIRS VERSUS MODISA COMPATIBILITY WITH
DIFFERENT ALGORITHMS: STANDARD NASA OC3 *chlor_a*,
EMPIRICAL FIT TO *In Situ* CHLA MATCH-UPS, AND THE OPTIMIZED
CHLA ALGORITHM. THE STATISTICS WITH SIGNIFICANT
IMPROVEMENT ARE SHOWN IN BOLD

Algorithm	R^2	MdAPE, %	MdRPE, %	RMSE	RmaSlope
Standard	0.95	13.7	-9.4	0.105	1.04
<i>In situ</i> fit	0.94	14.0	-6.8	0.125	1.12
Optimized	0.95	10.3	-0.1	0.113	1.04

TABLE III
POLYNOMIAL COEFFICIENTS OF THE OPTIMIZED CHLA ALGORITHM
(CALFIT2015) FOR MODISA AND VIIRS

Sensor	a_0	a_1	a_2	a_3	a_4
MODISA	0.327711	-3.44875	3.031143	-0.42728	-1.45675
VIIRS	0.442695	-3.65908	2.31464	2.369933	-3.41648

the derived Chla estimates were then minimized for the in- 182
put vector consisting of 24 MODISA bracket points of MBR 183
and Cins, 20 VIIRS bracket points of MBR and Cins, and 184
89 bracket points of MBR from MODISA and VIIRS. For 185
this optimization, we used the trust-region method, a variant 186
of the Levenberg–Marquardt method as implemented in the 187
NMath numerical libraries (<http://www.centerspace.net/>). As a 188
result, we produced two sets of polynomial coefficients (for 189
both MODISA and VIIRS) of the MBR OC3 model called 190
CALFIT2015 (Table III). 191

The optimization reduced the bias (MdRPE) between Chla 192
derived with MODISA and VIIRS from -9.4% to practically 193
zero (Table II and Fig. 4). It also reduced somewhat the scat- 194
ter (MdUAPE) between MODISA and VIIRS from $\sim 14\%$ to 195
 10% . However, the other statistical indicators (R^2 , rmse, and 196
RmaSlope) were not improved. 197

IV. DISCUSSION

The resulting optimized Chla algorithm shows improved 199
performance compared to the standard OC3 algorithm and 200

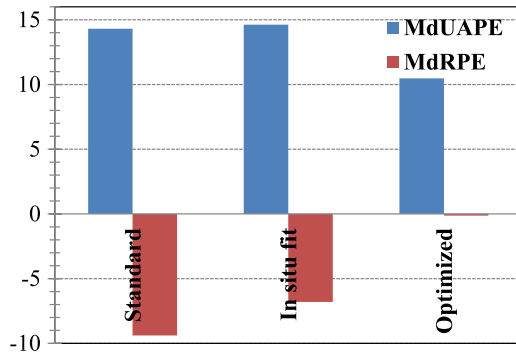


Fig. 4. Comparison of the differences between MODISA and VIIRS sensor-to-sensor match-ups: standard NASA *chlor_a* ("Standard"), empirical fit to the *in situ* Chla match-ups ("In situ fit"), and the optimized algorithm ("Optimized") showing the median unbiased percent error (MdUAPE) and the median relative percent error (MdrPE).

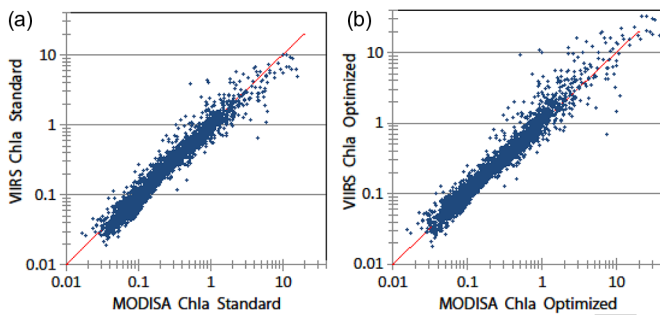


Fig. 5. VIIRS Chla versus MODISA Chla for a set of 4060 matching values of MBRs using the standard NASA *chlor_a* (a) and CALFIT2015 algorithm (b).

201 compared to the fit to *in situ* Chla match-ups. The observed
 202 underestimation of the standard OC3 algorithm at high *in situ*
 203 Chla was reduced, and the bias between Chla estimates by
 204 MODISA and VIIRS was eliminated (Table II and Fig. 4).
 205 The sensor-to-sensor scatter in Chla between MODISA and
 206 VIIRS was also somewhat reduced from 14% in the standard
 207 algorithm to 10% in the optimized algorithm. We also note
 208 that R^2 , rmse, and RmaSlope of the VIIRS versus MODISA
 209 compatibility were not improved (Table II). This is explained
 210 by the fact that the main effect of fitting to *in situ* data was
 211 the increase in Chla estimates at high Chla levels (Figs. 3 and
 212 5), but *Rrs* estimates corresponding to medium and high Chla
 213 are noisy [8]. Therefore, the scatter at high Chla was boosted,
 214 which inevitably made some of the statistics worse (e.g., rmse).
 215 As the median bias between MODISA and VIIRS has been
 216 eliminated, we can now merge Chla estimates from MODISA
 217 and VIIRS by simple arithmetic averaging of the gridded data
 218 and increase the frequency and spatial coverage and reduce
 219 uncertainty. However, we have to keep in mind that we have
 220 removed just the mean bias, and there may still exist bias
 221 between sensors related to factors such as sun zenith angle,
 222 sensor zenith angle, distance from the coast, etc. This has been
 223 discussed in [5] in the context of satellite-derived water clarity.

224

V. CONCLUSION

225 We have extended the optimization approach of [1] to current
 226 MODISA and VIIRS satellite data using a large database of

in situ Chla and produced updated versions of the region-
 227 ally optimized Chla algorithms. The new Chla estimates from
 228 MODISA and VIIRS are similar to standard *chlor_a* estimates
 229 at low Chla but have improved retrievals at medium to high
 230 *in situ* Chla and have no bias between one another. The
 231 improved algorithms (CALFIT2015) have been applied to
 232 MODISA and VIIRS imagery from 2012 to the present (2015).
 233 The merged satellite time series (available at [http://spg.ucsd.](http://spg.ucsd.edu/Satellite_Data/CC4km/CC4km.htm)
 234 [edu/Satellite_Data/CC4km/CC4km.htm](http://spg.ucsd.edu/Satellite_Data/CC4km/CC4km.htm)) have improved spatial
 235 and temporal coverage compared to a single sensor and im-
 236 proved correspondence to *in situ* data. Improved detection of
 237 high biomass events is crucial for running harmful algal bloom
 238 predictive models in coastal California that require accurate
 239 *Rrs* and chlorophyll values [10] and is also necessary to
 240 enhance our understanding of coastal biology and provide long-
 241 term continuity of ocean data records. 242

ACKNOWLEDGMENT

The authors would like to thank the CalCOFI program and
 244 Dr. R. Goericke for providing the *in situ* Chla data. Satellite data
 245 were provided by the NASA Ocean Color Processing Group. 246

REFERENCES

- [1] M. Kahru, R. M. Kudela, M. Manzano-Sarabia, and B. G. Mitchell, "Trends in the surface chlorophyll of the California Current: Merging data from multiple ocean color satellites," *Deep Sea Res. II, Top. Stud. Oceanogr.*, vol. 77–80, pp. 89–98, Nov. 2012. 248
- [2] S. Maritorena and D. A. Siegel, "Consistent merging of satellite ocean color data sets using a bio-optical model," *Remote Sens. Environ.*, vol. 94, no. 4, pp. 429–440, Feb. 2005. 252
- [3] W. W. Gregg, N. W. Casey, J. E. O'Reilly, and W. E. Esaias, "An empirical approach to ocean color data: Reducing bias and the need for post-launch radiometric re-calibration," *Remote Sens. Environ.*, vol. 113, no. 8, pp. 1598–1612, Aug. 2009. 255
- [4] C. Hu and C. Le, "Ocean color continuity from VIIRS measurements over Tampa Bay," *IEEE Geosci. Remote Sens. Lett.*, vol. 11, no. 5, pp. 945–949, May 2014. 259
- [5] B. B. Barnes and C. Hu, "Cross-sensor continuity of satellite-derived water clarity in the Gulf of Mexico: Insights into temporal aliasing and implications for long-term water clarity assessment," *IEEE Trans. Geosci. Remote Sens.*, vol. 53, no. 4, pp. 1761–1772, Apr. 2015. 262
- [6] B. A. Franz, S. W. Bailey, J. P. Werdell, and C. R. McClain, "Sensor-independent approach to the vicarious calibration of satellite ocean color radiometry," *Appl. Opt.*, vol. 46, no. 22, pp. 5068–5082, Aug. 2007. 266
- [7] C. Hu, L. Feng, and Z. Lee, "Uncertainties of SeaWiFS and MODIS remote sensing reflectance: Implications from clear water measurements," *Remote Sens. Environ.*, vol. 133, pp. 168–182, Jun. 2013. 270
- [8] M. Kahru, R. M. Kudela, C. R. Anderson, M. Manzano-Sarabia, and B. G. Mitchell, "Evaluation of satellite retrievals of ocean chlorophyll-a in the California Current," *Remote Sens.*, vol. 6, no. 9, pp. 8524–8540, Sep. 2014. 273
- [9] M. Szeto, J. P. Werdell, T. S. Moore, and J. W. Campbell, "Are the world's oceans optically different?" *J. Geophys. Res.*, vol. 116, no. C7, Jul. 2011, Art. ID. C00H04. 276
- [10] C. R. Anderson *et al.*, "Detecting toxic diatom blooms from ocean color and a regional ocean model," *Geophys. Res. Lett.*, vol. 38, no. 4, Feb. 2011, Art. ID. L04603. 279
- [11] M. D. Ohman and E. L. Venrick, "CalCOFI in a changing ocean," *Oceanography*, vol. 16, no. 3, pp. 76–85, 2003. 282
- [12] J. E. O'Reilly *et al.*, "Ocean color chlorophyll algorithms for SeaWiFS," *J. Geophys. Res.*, vol. 103, no. C11, pp. 24 937–24 953, Oct. 1998. 284
- [13] J. P. Werdell and S. W. Bailey, "An improved *in-situ* bio-optical data set for ocean color algorithm development and satellite data product validation," *Remote Sens. Environ.*, vol. 98, no. 1, pp. 122–140, Sep. 2005. 286
- [14] S. W. Bailey and J. P. Werdell, "A multi-sensor approach for the on-orbit validation of ocean color satellite data products," *Remote Sens. Environ.*, vol. 102, no. 1/2, pp. 12–23, May 2006. 289

AUTHOR QUERIES

AUTHOR PLEASE ANSWER ALL QUERIES

Please be aware that authors are required to pay overlength page charges (\$200 per page) if the paper is longer than 3 pages. If you cannot pay any or all of these charges please let us know.

This pdf contains 2 proofs. The first half is the version that will appear on Xplore. The second half is the version that will appear in print. If you have any figures to print in color, they will be in color in both proofs.

The “Open Access” option for your paper expires when the paper is published on Xplore in an issue with page numbers. Papers in “Early Access” may be changed to “Open Access.”

AQ1 = Please provide publication update in Ref. [14].

END OF ALL QUERIES

IEEE
PROOF

Optimized Merger of Ocean Chlorophyll Algorithms of MODIS-Aqua and VIIRS

Mati Kahru, Raphael M. Kudela, Clarissa R. Anderson, and B. Greg Mitchell

Abstract—Standard ocean chlorophyll-a (Chla) products from currently operational satellite sensors Moderate Resolution Imaging Spectroradiometer (MODIS) Aqua and Visible Infrared Imager Radiometer Suite (VIIRS) underestimate medium and high *in situ* Chla concentrations and have approximately 9% bias between each other in the California Current. By using the regional optimization approach of Kahru *et al.*, we minimized the differences between satellite estimates and *in situ* match-ups as well as between estimates of the two satellite sensors and created improved empirical algorithms for both sensors. The regionally optimized Chla estimates from MODIS-Aqua and VIIRS have no bias between each other, have improved retrievals at medium to high *in situ* Chla, and can be merged to improve temporal frequency and spatial coverage and to extend the merged time series.

Index Terms—Chlorophyll, Moderate Resolution Imaging Spectroradiometer (MODIS), ocean color, phytoplankton, Visible Infrared Imager Radiometer Suite (VIIRS).

I. INTRODUCTION

COMBINING or merging data from multiple sensors is required to improve the temporal resolution and spatial coverage of ocean color imagery and to construct long time series or climate data records using data from multiple sensors [2]–[5]. Currently (i.e., in mid-2015), there are two well-calibrated global ocean color sensors in operation: Moderate Resolution Imaging Spectroradiometer on Aqua (MODISA) and Visible Infrared Imager Radiometer Suite (VIIRS) on Suomi NPP. While improvements in on-orbit sensor calibration [6] have greatly improved the compatibility between data from different sensors, significant differences remain [7], [8]. Moreover, global algorithms may not be regionally optimal as significant differences exist in bio-optical properties of different oceanic provinces [9]. Standard NASA ocean chlorophyll-a (Chla) algorithms significantly underestimate *in situ* values in the California Current at high concentrations, often by a factor

of 5 [1]. This is highly relevant for detection and monitoring of phytoplankton blooms, including harmful algal blooms [10]. While differences between Chla estimates from MODIS-Aqua and VIIRS have diminished after multiple reprocessings, they still exist [8].

Kahru *et al.* [1] created optimized empirical algorithms for the California Current for a suite of four sensors (OCTS, SeaWiFS, MERIS, and MODISA) and the time period of 1997–2011. An update to that work is currently needed as 1) MERIS stopped operating in April 2012; 2) new data from VIIRS are available from the beginning of 2012; and 3) both MODISA and VIIRS data have been reprocessed by NASA's Ocean Biology Processing Group. The purpose of this work is to create empirical algorithms that are optimized for creating a merged Chla time series in the California Current for the period of 2012–2015 from the two currently available sensors MODISA and VIIRS.

II. DATA AND METHODS

We used *in situ* Chla data collected by the California Cooperative Oceanic Fisheries Investigations (CalCOFI) on their quarterly cruises covering a regular grid of stations from nearshore to as far as 600 km offshore for the entire coast of California [11]. In total, 3388 near-surface Chla samples from 2002–2014 were used to validate MODISA data, and 744 Chla samples from 2012–2014 were used to validate VIIRS data.

All satellite data were acquired at level 2 (i.e., processed to surface quantities but unmapped) with approximately 1-km ground resolution. MODISA (2002–2014, version 2013.1.1) and VIIRS (2012–2014, version 2014.0.1) level-2 data were obtained from NASA's Ocean Color Web (<http://oceancolor.gsfc.nasa.gov/>). The standard NASA Chla algorithm uses empirical polynomial fits between satellite-derived maximum band ratio (MBR) of remote sensing reflectance (R_{rs}) bands and near-surface Chla [12] with the coefficient values for each sensor given at http://oceancolor.gsfc.nasa.gov/cms/atbd/chlor_a.

The validation of satellite products using quasi-simultaneous and spatially collocated measurements (match-ups) of satellite and *in situ* data followed the procedures of previous studies [1], [8], [13], [14]. We assumed that the following level-2 flags made a pixel invalid: ATMFAIL, LAND, HISATZEN, STRAYLIGHT, CLDICE, CHLFAIL, SEAICE, NAVFAIL, and HIPOL (see <http://oceancolor.gsfc.nasa.gov/VALIDATION/80flags.html> for an explanation of the flags). All variables in the level-2 files were extracted from a 3×3 -pixel window centered at the pixel nearest to the *in situ* sample. For statistical analysis, we accepted only those match-ups with at least five

Manuscript received May 28, 2015; revised July 9, 2015; accepted August 17, 2015. This work was supported by the NASA Ocean Biology and Biogeochemistry Program Grants NNX09AT01G (M. Kahru and R. M. Kudela), NNX13AL28G (C. R. Anderson, R. M. Kudela, and M. Kahru), and NNX14AC42G (C. R. Anderson and R. M. Kudela) and by the National Science Foundation (Grant OCE-1026607 to the CCE-LTER Program).

M. Kahru and B. G. Mitchell are with Scripps Institution of Oceanography, University of California, San Diego, La Jolla, CA 95064 USA (e-mail: mkahru@ucsd.edu; gmitchell@ucsd.edu).

R. M. Kudela and C. R. Anderson are with the Ocean Sciences Department, University of California, Santa Cruz, Santa Cruz, CA 95064 USA (e-mail: kudela@ucsc.edu; clrande@ucsc.edu).

Color versions of one or more of the figures in this paper are available online at <http://ieeexplore.ieee.org>.

Digital Object Identifier 10.1109/LGRS.2015.2470250

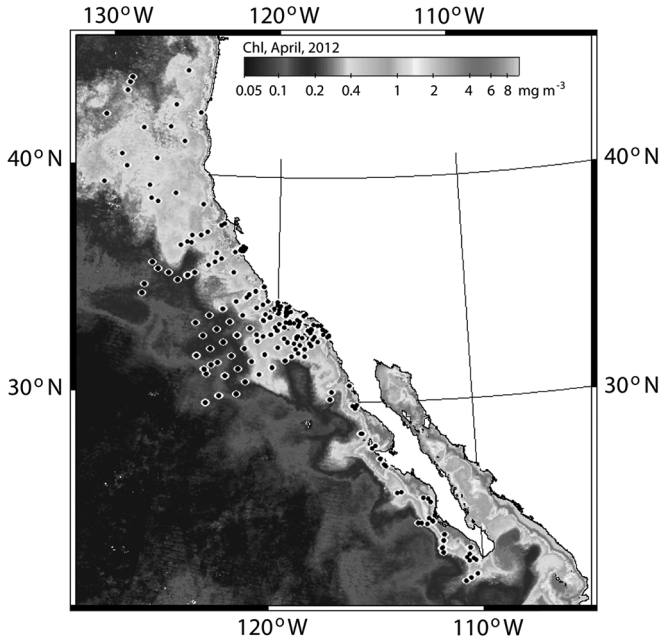


Fig. 1. Locations of the MODIS-Aqua Chla match-ups (black dots with white circles) within 3-h time difference overlaid on the April 2012 Chla composite.

85 valid pixels (out of nine). The maximum temporal difference 86 between satellite and *in situ* measurements was set at 3 h. 87 Satellite match-ups with high variability within the 3×3 -pixel 88 window were excluded if $(\text{Max} - \text{Min})/\text{Min} > 0.6$ for the 89 standard Chla variable *chlora*. The arithmetic mean Chla value 90 of all valid pixels within the 3×3 -pixel window was used as the 91 satellite retrieval. The spatial distribution of MODISA match- 92 ups with *in situ* measurements of Chla is shown in Fig. 1.

93 Satellite-derived *Rrs* values between different sensors are 94 difficult to compare at level 2, i.e., without remapping to a com- 95 mon map. Although both MODISA and VIIRS have equatorial 96 crossing times at approximately 1:30 P.M., their pixel-to-pixel 97 comparison at a spatial resolution of $\sim 1 \text{ km}^2$ corresponding 98 to their level-2 data shows high variability [8]. We therefore 99 used spatially binned and averaged *Rrs* values over a grid of 100 1° latitude \times 1° longitude covering an approximately 1000-km- 101 wide area along the coast extracted from daily NASA level-3 102 datasets. Those daily mean *Rrs* values of MODISA and VIIRS 103 were then matched with each other. In order to eliminate cloud 104 edges and coastal zones, we kept only those matching *Rrs* pairs 105 with at least 99% of the pixels within each $1^\circ \times 1^\circ$ subarea 106 having valid values. As a result, a total of 4060 matching *Rrs* 107 vectors for MODISA and VIIRS were found for the period 108 of 2012–2014. These MODISA to VIIRS match-ups were 109 then used in the minimization of the differences in the Chla 110 algorithm between MODISA and VIIRS.

111 Several statistical measures were used to assess the per- 112 formance of satellite products against *in situ* observations 113 and between different satellite sensors. For satellite to *in situ* 114 match-ups, we assume that O_i is the i th observation of an *in situ* 115 variable and P_i is the corresponding predicted satellite variable. 116 For sensor-to-sensor match-ups, the choice of the observed 117 versus predicted variable is arbitrary, but we used MODISA 118 estimates as O_i . As an estimate of the prediction scatter, we

TABLE I
STATISTICS FOR MATCH-UPS OF THE NASA STANDARD *chlora* PRODUCT WITH *In Situ* CHLA WITH UP TO 3-h TIME DIFFERENCE AND AT LEAST FIVE VALID PIXELS. N = NUMBER OF MATCH-UPS, R^2 = COEFFICIENT OF DETERMINATION, MDAPE = MEDIAN ABSOLUTE PERCENT ERROR, MDRPE = MEDIAN RELATIVE PERCENT ERROR, RMSE = ROOT MEAN SQUARE ERROR, AND RMA SLOPE = SLOPE OF THE RMA LINEAR REGRESSION

Sensor	N	R^2	MdAPE	MdRPE	RMSE	RmaSlope
MODISA	306	0.87	22.5	-0.1	0.15	0.88
VIIRS	74	0.85	31.0	8.0	0.21	0.68

used the median absolute percentage error (MdAPE), which 119 was calculated as $\text{MdAPE} = 100 \times \text{median} (|(P_i - O_i)/O_i|)$. 120 For comparing two sensors, we used the median unbiased 121 absolute percentage error (MdUAPE), which was calculated as 122 $\text{MdUAPE} = 100 \times \text{median} (|(P_i - O_i)/[0.5*(P_i + O_i)]|)$. As 123 an estimate of bias, we used the median relative percentage 124 error (MdRPE), which was calculated as $\text{MdRPE} = 100 \times$ 125 $\text{median} ((P_i - O_i)/O_i)$. These statistics were calculated for 126 P_i and O_i using untransformed values (i.e., not \log_{10}). We 127 also include the coefficient of determination (R^2), the slope 128 of the reduced major axis (RMA) regression, and the root- 129 mean-square error (rmse), all calculated on \log_{10} -transformed 130 variables. 131

III. RESULTS 132

A. Match-Ups With Standard *chlora* Products 133

Satellite to *in situ* match-ups of Chla using the NASA stan- 134 dard *chlora* product over three orders of magnitude (Fig. 2 and 135 Table I) have relatively high coefficients of determination 136 ($R^2 = 0.87$ for MODISA and 0.85 for VIIRS) but also show 137 bias. For example, all MODISA match-ups with *in situ* Chla $>$ 138 2 mg m^{-3} underestimate *in situ* Chla. For VIIRS, the standard 139 *chlora* product suffers from overestimation at low *in situ* Chla 140 and underestimation at medium and high Chla, which causes 141 the slope of the RMA regression to be significantly less than 142 one (0.68; Table I). 143

B. Optimized MBR Algorithm 144

Standard empirical ocean color algorithms OC3 and OC4 145 [12] use polynomial fits between \log_{10} -transformed *in situ* 146 Chla (Cins) and \log_{10} -transformed MBR of *Rrs* measured 147 *in situ*. MBR is calculated as the maximum of *Rrs* at two or 148 more wavelengths (e.g., *Rrs*443 and *Rrs*488 for MODISA or 149 *Rrs*443 and *Rrs*486 for VIIRS) to the *Rrs* of the green band 150 (*Rrs*547 for MODISA and *Rrs*551 for VIIRS). In order to 151 remove the bias evident in Fig. 2, we created our own best 152 fits to the match-up points. The distribution of match-up points 153 is highly uneven as there are more points in the middle of the 154 range than at both ends of the distribution. To reduce the effect 155 of the uneven distribution, the match-up points were aggregated 156 into bins by using the median values of small brackets of 157 $\log_{10}(\text{Cins})$ and the corresponding medians of $\log_{10}(\text{MBR})$ 158 following [3] and binning interval of 0.04 in $\log_{10}(\text{MBR})$ units. 159

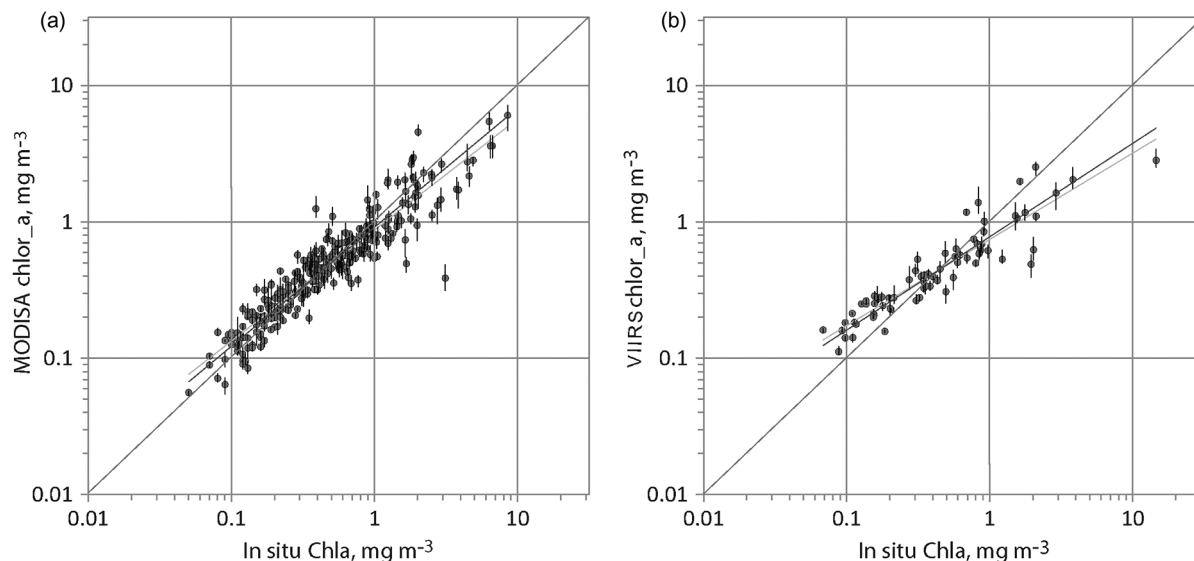


Fig. 2. Chlorophyll-a match-ups with (a) MODISA and (b) VIIRS using standard NASA *chlor_a* products. The red line is the one-to-one line, and the blue line is the RMA linear regression.

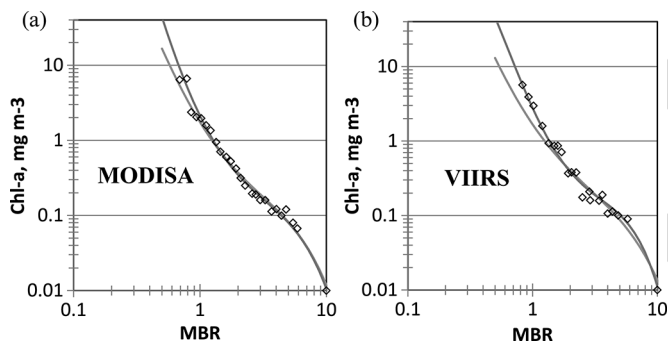


Fig. 3. Optimized Chla algorithm (red) compared to standard NASA OC3 (blue) and bracket points of *in situ* Chla match-ups (black diamonds) as a function of the MBR of remote sensing reflectance for (a) MODISA and (b) VIIRS.

160 The resulting “bracket” points (24 for MODISA and 20 for
161 VIIRS) were then used in algorithm development (Fig. 3).

162 Ideally, by “tuning” the algorithms of multiple sensors to the
163 same set of *in situ* data, the resulting estimates by different
164 sensors should be compatible between each other. In reality, as
165 the Chla high end is poorly constrained due to few scattered
166 match-ups, the resulting empirical algorithms do not improve
167 the intersensor consistency and may even make it worse [1].
168 Indeed, as the main difference of the empirical fits compared
169 to the standard OC3 algorithms is their increased predicted
170 Chla at high end (Fig. 3), the intersensor variability (MdAPE)
171 between MODISA and VIIRS is slightly increased from 13.7%
172 to 14.0% when using the coefficients fitted to *in situ* data
173 (Table II). In order to improve the consistency between satellite
174 sensors and at the same time keep them consistent with *in situ*
175 datasets, we need an optimization that minimizes not only the
176 differences between satellite and *in situ* match-ups but also the
177 differences between the satellite estimates of different sensors
178 [1]. The matching *Rrs* pairs of MODISA and VIIRS in $1^\circ \times 1^\circ$
179 subareas were further binned according to the corresponding
180 $\log_{10}(\text{MBR})$ value, which resulted in 89 “bracket points” of
181 MODISA and VIIRS $\log_{10}(\text{MBR})$ values. The differences in

TABLE II
STATISTICS OF VIIRS VERSUS MODISA COMPATIBILITY WITH
DIFFERENT ALGORITHMS: STANDARD NASA OC3 *chlor_a*,
EMPIRICAL FIT TO *In Situ* CHLA MATCH-UPS, AND THE OPTIMIZED
CHLA ALGORITHM. THE STATISTICS WITH SIGNIFICANT
IMPROVEMENT ARE SHOWN IN BOLD

Algorithm	R^2	MdAPE, %	MdRPE, %	RMSE	RmaSlope
Standard	0.95	13.7	-9.4	0.105	1.04
<i>In situ</i> fit	0.94	14.0	-6.8	0.125	1.12
Optimized	0.95	10.3	-0.1	0.113	1.04

TABLE III
POLYNOMIAL COEFFICIENTS OF THE OPTIMIZED CHLA ALGORITHM
(CALFIT2015) FOR MODISA AND VIIRS

Sensor	a_0	a_1	a_2	a_3	a_4
MODISA	0.327711	-3.44875	3.031143	-0.42728	-1.45675
VIIRS	0.442695	-3.65908	2.31464	2.369933	-3.41648

the derived Chla estimates were then minimized for the in- 182
put vector consisting of 24 MODISA bracket points of MBR 183
and Cins, 20 VIIRS bracket points of MBR and Cins, and 184
89 bracket points of MBR from MODISA and VIIRS. For 185
this optimization, we used the trust-region method, a variant 186
of the Levenberg–Marquardt method as implemented in the 187
NMath numerical libraries (<http://www.centerspace.net/>). As a 188
result, we produced two sets of polynomial coefficients (for 189
both MODISA and VIIRS) of the MBR OC3 model called 190
CALFIT2015 (Table III). 191

The optimization reduced the bias (MdRPE) between Chla 192
derived with MODISA and VIIRS from -9.4% to practically 193
zero (Table II and Fig. 4). It also reduced somewhat the scat- 194
ter (MdUAPE) between MODISA and VIIRS from $\sim 14\%$ to 195
 10% . However, the other statistical indicators (R^2 , rmse, and 196
RmaSlope) were not improved. 197

IV. DISCUSSION

The resulting optimized Chla algorithm shows improved 199
performance compared to the standard OC3 algorithm and 200

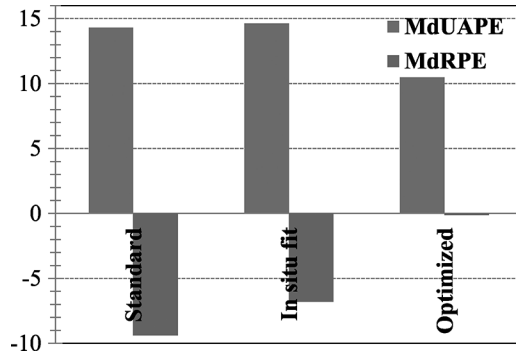


Fig. 4. Comparison of the differences between MODISA and VIIRS sensor-to-sensor match-ups: standard NASA *chlor_a* (“Standard”), empirical fit to the *in situ* Chla match-ups (“In situ fit”), and the optimized algorithm (“Optimized”) showing the median unbiased percent error (MdUAPE) and the median relative percent error (MdRPE).

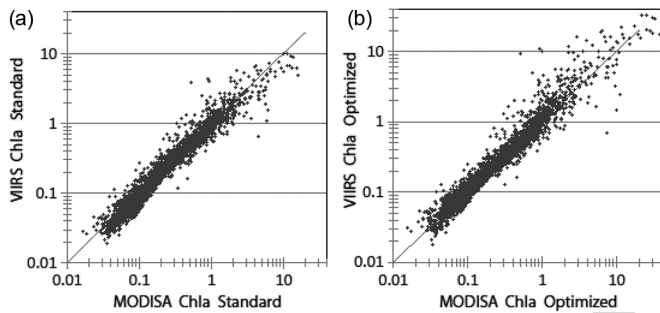


Fig. 5. VIIRS Chla versus MODISA Chla for a set of 4060 matching values of MBRs using the standard NASA *chlor_a* (a) and CALFIT2015 algorithm (b).

201 compared to the fit to *in situ* Chla match-ups. The observed
 202 underestimation of the standard OC3 algorithm at high *in situ*
 203 Chla was reduced, and the bias between Chla estimates by
 204 MODISA and VIIRS was eliminated (Table II and Fig. 4).
 205 The sensor-to-sensor scatter in Chla between MODISA and
 206 VIIRS was also somewhat reduced from 14% in the standard
 207 algorithm to 10% in the optimized algorithm. We also note
 208 that R^2 , rmse, and RmaSlope of the VIIRS versus MODISA
 209 compatibility were not improved (Table II). This is explained
 210 by the fact that the main effect of fitting to *in situ* data was
 211 the increase in Chla estimates at high Chla levels (Figs. 3 and
 212 5), but *Rrs* estimates corresponding to medium and high Chla
 213 are noisy [8]. Therefore, the scatter at high Chla was boosted,
 214 which inevitably made some of the statistics worse (e.g., rmse).
 215 As the median bias between MODISA and VIIRS has been
 216 eliminated, we can now merge Chla estimates from MODISA
 217 and VIIRS by simple arithmetic averaging of the gridded data
 218 and increase the frequency and spatial coverage and reduce
 219 uncertainty. However, we have to keep in mind that we have
 220 removed just the mean bias, and there may still exist bias
 221 between sensors related to factors such as sun zenith angle,
 222 sensor zenith angle, distance from the coast, etc. This has been
 223 discussed in [5] in the context of satellite-derived water clarity.

224

V. CONCLUSION

225 We have extended the optimization approach of [1] to current
 226 MODISA and VIIRS satellite data using a large database of

in situ Chla and produced updated versions of the region-
 227 ally optimized Chla algorithms. The new Chla estimates from
 228 MODISA and VIIRS are similar to standard *chlor_a* estimates
 229 at low Chla but have improved retrievals at medium to high
 230 *in situ* Chla and have no bias between one another. The
 231 improved algorithms (CALFIT2015) have been applied to
 232 MODISA and VIIRS imagery from 2012 to the present (2015).
 233 The merged satellite time series (available at http://spg.ucsd.edu/Satellite_Data/CC4km/CC4km.htm) have improved spatial
 234 and temporal coverage compared to a single sensor and im-
 235 proved correspondence to *in situ* data. Improved detection of
 236 high biomass events is crucial for running harmful algal bloom
 237 predictive models in coastal California that require accurate
 238 *Rrs* and chlorophyll values [10] and is also necessary to
 239 enhance our understanding of coastal biology and provide long-
 240 term continuity of ocean data records.

242

ACKNOWLEDGMENT

243

The authors would like to thank the CalCOFI program and
 244 Dr. R. Goericke for providing the *in situ* Chla data. Satellite data
 245 were provided by the NASA Ocean Color Processing Group.

246

REFERENCES

247

- [1] M. Kahru, R. M. Kudela, M. Manzano-Sarabia, and B. G. Mitchell, “Trends in the surface chlorophyll of the California Current: Merging data from multiple ocean color satellites,” *Deep Sea Res. II, Top. Stud. Oceanogr.*, vol. 77–80, pp. 89–98, Nov. 2012. 248
- [2] S. Maritorena and D. A. Siegel, “Consistent merging of satellite ocean color data sets using a bio-optical model,” *Remote Sens. Environ.*, vol. 94, no. 4, pp. 429–440, Feb. 2005. 252
- [3] W. W. Gregg, N. W. Casey, J. E. O’Reilly, and W. E. Esaias, “An empirical approach to ocean color data: Reducing bias and the need for post-launch radiometric re-calibration,” *Remote Sens. Environ.*, vol. 113, no. 8, pp. 1598–1612, Aug. 2009. 255
- [4] C. Hu and C. Le, “Ocean color continuity from VIIRS measurements over Tampa Bay,” *IEEE Geosci. Remote Sens. Lett.*, vol. 11, no. 5, pp. 945–949, May 2014. 256
- [5] B. B. Barnes and C. Hu, “Cross-sensor continuity of satellite-derived water clarity in the Gulf of Mexico: Insights into temporal aliasing and implications for long-term water clarity assessment,” *IEEE Trans. Geosci. Remote Sens.*, vol. 53, no. 4, pp. 1761–1772, Apr. 2015. 262
- [6] B. A. Franz, S. W. Bailey, J. P. Werdell, and C. R. McClain, “Sensor-independent approach to the vicarious calibration of satellite ocean color radiometry,” *Appl. Opt.*, vol. 46, no. 22, pp. 5068–5082, Aug. 2007. 263
- [7] C. Hu, L. Feng, and Z. Lee, “Uncertainties of SeaWiFS and MODIS remote sensing reflectance: Implications from clear water measurements,” *Remote Sens. Environ.*, vol. 133, pp. 168–182, Jun. 2013. 264
- [8] M. Kahru, R. M. Kudela, C. R. Anderson, M. Manzano-Sarabia, and B. G. Mitchell, “Evaluation of satellite retrievals of ocean chlorophyll-a in the California Current,” *Remote Sens.*, vol. 6, no. 9, pp. 8524–8540, Sep. 2014. 271
- [9] M. Szeto, J. P. Werdell, T. S. Moore, and J. W. Campbell, “Are the world’s oceans optically different?” *J. Geophys. Res.*, vol. 116, no. C7, Jul. 2011, Art. ID. C00H04. 276
- [10] C. R. Anderson *et al.*, “Detecting toxic diatom blooms from ocean color and a regional ocean model,” *Geophys. Res. Lett.*, vol. 38, no. 4, Feb. 2011, Art. ID. L04603. 277
- [11] M. D. Ohman and E. L. Venrick, “CalCOFI in a changing ocean,” *Oceanography*, vol. 16, no. 3, pp. 76–85, 2003. 282
- [12] J. E. O’Reilly *et al.*, “Ocean color chlorophyll algorithms for SeaWiFS,” *J. Geophys. Res.*, vol. 103, no. C11, pp. 24 937–24 953, Oct. 1998. 283
- [13] J. P. Werdell and S. W. Bailey, “An improved *in-situ* bio-optical data set for ocean color algorithm development and satellite data product validation,” *Remote Sens. Environ.*, vol. 98, no. 1, pp. 122–140, Sep. 2005. 284
- [14] S. W. Bailey and J. P. Werdell, “A multi-sensor approach for the on-orbit validation of ocean color satellite data products,” *Remote Sens. Environ.*, vol. 102, no. 1/2, pp. 12–23, May 2006. 285

291 AQI

AUTHOR QUERIES

AUTHOR PLEASE ANSWER ALL QUERIES

Please be aware that authors are required to pay overlength page charges (\$200 per page) if the paper is longer than 3 pages. If you cannot pay any or all of these charges please let us know.

This pdf contains 2 proofs. The first half is the version that will appear on Xplore. The second half is the version that will appear in print. If you have any figures to print in color, they will be in color in both proofs.

The “Open Access” option for your paper expires when the paper is published on Xplore in an issue with page numbers. Papers in “Early Access” may be changed to “Open Access.”

AQ1 = Please provide publication update in Ref. [14].

END OF ALL QUERIES

IEEE
PROOF